SCIEPublish

Article

Partial Duration Series of Wet and Dry Years Can Improve Flood Estimates in the Context of a Nonstationary Climate and Anthropogenic Disturbances

Rouzbeh Berton [1,*] and Vahid Rahmani [2]

[1] Stantec Consulting Inc., 410 17th St #1500, Denver, CO 80202, USA

[2] Department of Biological and Agricultural Engineering, Kansas State University, 1016 Seaton Hall, 920 N. Martin Luther King, Jr. Drive, Manhattan, KS 66506, USA; VRahmani@ksu.edu (V.R.)

* Corresponding author. E-mail: rouzbeh.berton@stantec.com (R.B.)

Received: 1 October 2024; Accepted: 21 November 2024; Available online: 25 November 2024

ABSTRACT: Accurately estimating flood levels is essential for effective infrastructure design, reservoir management, and flood risk mapping. Traditional methods for predicting these levels often rely on annual maximum flood (AMF) data, which may not always fit well to statistical models. To improve these estimates, we tested an approach that considers floods in relation to annual climate conditions—specifically, average, wet, and dry years—using daily streamflow data. We examined how well the Log Pearson Type III (LP3) distribution, a commonly used statistical model in flood frequency analysis, estimates flood levels when applied to these customized datasets instead of standard AMF data. Our study included over 70 years of data from 2028 basins across the United States, with drainage areas ranging from small (4.0 km^2) to large (50,362 km^2). We found that in some regions, LP3 better estimated frequent floods (recurrence interval of 2 to 25 years) when applied to AMF data. However, for less frequent, larger floods (recurrence interval of 50 to 200 years), the LP3 model worked better when applied to datasets representing wet or dry years. This approach could lead to more reliable flood predictions, which would benefit infrastructure planning and flood preparedness efforts.

Keywords: Flood frequency analysis; Partial duration series; Annual maximum flood; Wet and dry years; Log Pearson Type III (LP3); Reference site; Nonreference site; United States

1. Introduction

High quantile precipitation has been increased across the United States [1–3]. This increase may be a result of rising global air temperature, which allows the atmosphere to hold more moisture [4–6]. Although the positive trends in the magnitude or frequency of high quantile precipitation may not directly translate into positive trends in streamflow [7–9], the likelihood of experiencing more intense precipitation increases the chance of flood hazards [10–14]. The extent of flood hazards and the associated risk to infrastructure will differ between rural and urbanized basins [15,16] as well as between inland and coastal regions [17,18]. Therefore, understanding the variations in flood frequency and magnitude is of great interest when studying floods in both undisturbed and anthropogenically disturbed watersheds located within coastal or inland water resources regions in the US.

In the US, most studies on flooding have utilized flood series based on the single highest streamflow values of each year, known as the annual maximum flood (AMF) [19–22]. Only a few studies considered partial duration series (PDS) instead of AMF to estimate flood quantiles [7,23–27]. With projections of a warmer and wetter climate for the 21st century [28–30], subsequent high flow events, in addition to the AMF in a wet year, may exceed the AMF of a dry year [31]. Therefore, combining AMF with a series of independent flooding events per year—also recognized as partial duration series (PDS)—presents an opportunity to better estimate flood quantiles [7,32–34]. Additionally, flooding events during average, wet, and dry years may arise from different mechanisms, so developing PDS for these years separately could further improve the estimation of both small and large flooding events.

https://doi.org/10.70322/hee.2024.10004

The Log Pearson Type III distribution (LP3), fitted to AMF, is a widely used statistical procedure recommended for flood frequency analysis [35–37]. When LP3 is applied to PDS of average, wet, and dry years, in addition to AMF, it can provide a better understanding of how flood estimates may vary, particularly during extreme wet and dry years [26,27,33]. The geographical extent where flooding events can be more accurately estimated using the PDS of wet and dry years, rather than AMF, may be influenced by the strength of large-scale atmospheric circulation patterns over the Pacific and Atlantic oceans [38–40]. Recognizing these influences on regional flooding can be valuable for flood risk management, helping to prepare for potential disastrous events.

In this study, we tested whether using PDS instead of AMF data could improve flood frequency estimates, depending on the region. With a warmer and wetter climate projected for the 21st century, high-flow events within a single wet year may exceed the AMF of a dry year. By combining AMF with multiple independent flood events each year, we may achieve better flood quantile estimates. Since floods during average, wet, and dry years can have different causes, creating separate PDS for these years could further enhance estimates for both frequent and rare flood events. To test our hypothesis, specifically, we: (1) developed separate PDS datasets for average, wet, and dry years using daily streamflow data; (2) evaluated the performance of the LP3 distribution when applied to PDS of wet and dry years, in comparison to AMF; and (3) examined differences in flood estimation between reference (undisturbed) and nonreference (disturbed) sites.

We analyzed 247 reference sites and 1781 nonreference sites, all with peak flow records of at least 70 years. We fitted LP3 to AMF and the PDS of average, wet, and dry years to estimate flooding events with return period of 2 to 200 years across 18 water resources regions (HUC02) identified for the conterminous United States. We compared the reliability of estimated flood quantiles for reference and nonreference sites within each region. This study offers an alternative approach to flood frequency analysis using AMF in regions where LP3 fits better with PDS derived from wet or dry years. The updated flood frequency analysis can provide critical information to reduce structural damage, protect human lives, and lower maintenance costs of existing infrastructures, while also supporting the sustainable design of new hydraulic systems and infrastructures.

2. Data

2.1. Annual Maximum Flood (AMF)

We selected 2028 out of 9067 U.S. Geological Survey (USGS) streamflow gaging stations that had more than 70 years of peak flow records and less than 5% missing daily flow values for each water year. We used the "Hydro-Climatic Data Network" (HCDN or Gages-II) [41] to identify reference sites within watersheds that have no or minimal anthropogenic disturbances. Nonreference sites, on the other hand, have a history of land use/cover change, regulated streams, and/or impoundments [42]. According to HCDN information, 247 streamflow gaging stations were classified as reference sites, while 1781 were classified as nonreference sites.

Figure 1 presents the spatial distribution of the study sites. Notably, sites with longer peak flow records are primarily located east of the 105th meridian. Additional information about the study sites can be found in the supplementary material section. The data were retrieved from the USGS National Water Information System (NWIS) data repository using the "dataRetrieval" [43] and "dplyr" [44] packages developed by USGS. The site selection and data cleaning processes were computer coded in "R" by the authors.

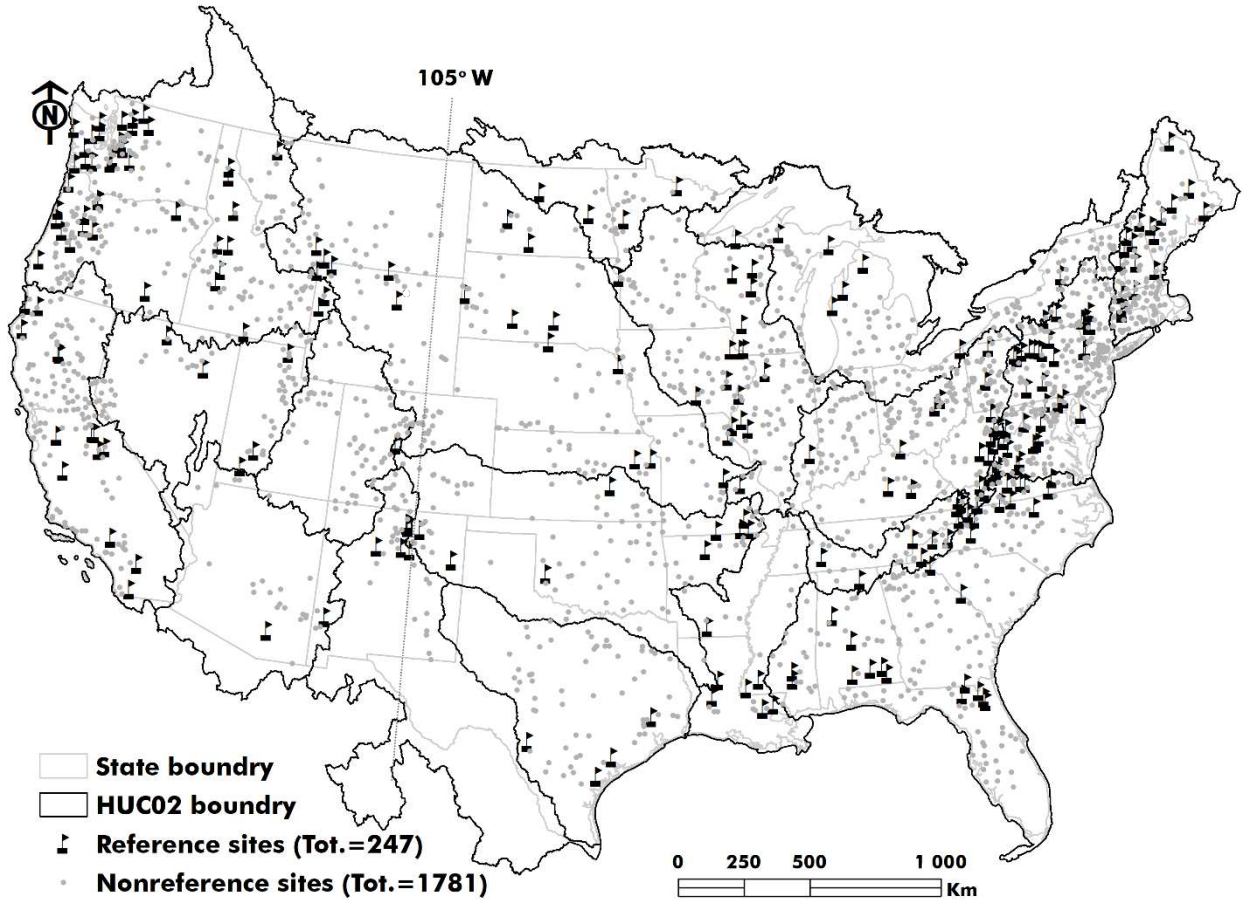

Figure 1. The spatial distribution of 247 reference (dark flags) and 1781 nonreference (gray circles) sites across the conterminous US. The water resources regions are defined by HUC02 hydrologic units, as determined by USGS.

2.2. Partial Duration Series (PDS)

The rationale for developing PDS lies in the possibility that some peak flow events in certain years may exceed the smallest peak flow in the AMF series. In such cases, PDS may provide a better representation of the statistical properties of the actual peak flow population. On average, one can expect to observe at least 4–5 independent peak flow events each year [45,46]. Since the selected peak flow events must be independent, and minimal constraint should be imposed, PDS can be derived from daily mean streamflow data [47].

In this study, we classified years into average, wet, and dry hydrologic conditions based on the criteria set by Genz and Luz (2012) [48]. We used a liberal approach, considering half the standard deviation from the long-term average to distinguish among average, wet, and dry years. In this approach, average years are defined as those where the total annual discharge falls within half a standard deviation above or below the long-term annual average discharge. If the total annual discharge for a specific year exceeded (or was less than) the long-term average plus (or minus) half a standard deviation, the year was classified as wet (or dry). After classification, we developed PDS separately for average, wet, and dry hydrologic conditions.

For each hydrologic condition, we selected mean daily flows that exceeded the smallest peak flow values in the AMF series. We identified all absolute and relative extrema in the mean daily streamflow record. To assess the independence of these extrema, we applied Flynn (1982) criteria [49], using the natural log of drainage area (in square miles) and adding a five-day interval to define independent flooding events. The record lengths for both the AMF and PDS series were provided in the supplementary materials. On average, the PDS derived from dry years contained more data records. While wet years often had multiple dependent flooding events, dry-year floods were typically not triggered by successive rainfall storms. This allowed peak flow events to be sufficiently spaced, making them independent. We developed R code to automate the generation of the PDS.

3. Method

The LP3 distribution is widely accepted and highly recommended for estimating flood quantiles, both nationally and globally [31,36,50]. We followed the LP3 product moment formulation outlined by Stedinger et al. (1993) [51]. No regional correction factor was applied to adjust for station skewness. Below, we provide a summary of the mathematical formulation used to determine the LP3 distribution parameters.

The Probability Density Function (PDF) for LP3 distribution could be written as:

$$f_X(X) = |\beta|\left[\beta\left(\ell n(X) - \xi\right)\right]^{\alpha-1} \frac{exp\left[-\beta\left(\ell n(X) - \xi\right)\right]}{X\,\Gamma(\alpha)} \tag{1}$$

where X in the natural log of the observed streamflow. The parameters of the LP3 distribution— shape (α), scale (β), and location (ξ)—can be computed using the mean ($\hat{\mu}_X$, first moment), variance ($\hat{\sigma}_X^2$, second moment), and skewness ($\hat{\gamma}_X$, third moment) of the observations:

$$\alpha = \frac{4}{\hat{\gamma}_X^2},\ \beta = \frac{2}{\hat{\sigma}_X \hat{\gamma}_X},\ \xi = \hat{\mu}_X - \frac{\alpha}{\beta} = \hat{\mu}_X - \frac{2\hat{\sigma}_X}{\hat{\gamma}_X} \text{ where} \tag{2}$$

$$\hat{\mu}_X = \bar{X} = \frac{1}{n}\sum_{i=1}^{n} X_i\ ,\hat{\sigma}_X^2 = S^2 = \frac{1}{n-1}\sum_{i=1}^{n}\left(X_i - \bar{X}\right)^2,\ \hat{\gamma}_X = \frac{n}{(n-1)(n-2)S^3}\sum_{i=1}^{n}\left(X_i - \bar{X}\right)^3 \tag{3}$$

The flood quantiles can be estimated as $X_P = \mu_Q + \sigma_Q K_P(\gamma_Q)$ where:

$$\mu_Q = e^{\xi}\left(\frac{\beta}{\beta-1}\right)^{\alpha},\ \sigma_Q^2 = e^{2\xi}\left[\left(\frac{\beta}{\beta-2}\right)^{\alpha} - \left(\frac{\beta}{\beta-1}\right)^{2\alpha}\right],\ E\left[Q^r\right] = e^{r\xi}\left(\frac{\beta}{\beta-r}\right)^{\alpha},$$
$$\gamma_Q = \frac{E\left[Q^3\right] - 3\mu_Q E\left[Q^2\right] + 2\mu_Q^3}{\sigma_Q^3},\ K_P(\gamma_Q) = \frac{2}{\gamma_Q}\left[1 + \frac{\gamma_Q Z_P}{6} - \frac{\gamma_Q^2}{36}\right]^3 - \frac{2}{\gamma_Q} \tag{4}$$

Z_P represents the P-th quantile of the standard normal distribution, which can be numerically estimated as follows:

$$Z_P = \frac{P^{0.135} - (1-P)^{0.135}}{0.1975} \text{ for } P > 0.5 \tag{5}$$

The goodness-of-fit for the LP3 distribution is tested using the Blom empirical probability formula (Blom, 1958 [52]):

$$P_i = 1 - \frac{i - 0.375}{n + 0.25} \tag{6}$$

where $i = 1$ represents the greatest peak flow ranked, and "n" is the total number of observations. The reliable performance of the LP3 distribution is confirmed when the plot of $K_{P_i}(\gamma_Q)$ against the anomalies of the observations $Z_i = \frac{X_i - \bar{X}}{\sigma_X}$ falls along the 1:1 line (Serago and Vogel, 2018 [33]).

4. Results and Discussion

The results are presented for floods with return periods of 2, 5, 10, 25, 50, 100, and 200 years. We focus on sites where flood quantile estimates are reliable, indicated by an observed-to-estimated flood ratio (R < 1) when fitting LP3 to AMF or PDS for average, wet, or dry years. This ratio is further discussed in the next section. The patterns are analyzed within the HUC02 water resources regions [53].

4.1. Performance of LP3 Distribution Fitted to the AMF and PDS

We identified four main scenarios for LP3 applied to AMF and PDS, depending on flood genesis in the region. When the peak instantaneous daily streamflow exceeded daily average, PDS based on average flows produced lower flood quantiles estimates than AMF (Figure 2a–c). In contrast, if the PDS for wet years included peak flows similar to those in AMF, LP3 applied to PDS provided higher estimates for low-frequency floods (e.g., 100 years or greater) than LP3 applied to AMF (Figure 2d).

Although PDS is typically assumed to vary by wet, average, and dry years, we found that the largest flood could occur in any of these conditions. For instance, in Figure 2a, the PDS for average years stays above those for wet and dry years as the return period increases. In Figure 2b, a 100-year flood in the PDS for dry years remains higher than that of wet and average years. In Figure 2c, as return periods increase, the PDS for dry years is higher than for average years but lower than for wet years. Figure 2d shows the PDS for wet years exceeding those for both average and dry years.

The goodness-of-fit test assesses how well the LP3 distribution estimates flood quantiles (e.g., Serago and Vogel, 2018 [33]). We applied this test to LP3 fitted to both AMF and PDS data, with results shown in Table 1 for reference and nonreference sites. The Pearson cross-correlation values of "$Z_i = \frac{X_i - \overline{X}}{\sigma_X}$" with "$K_{P_i}\left(\gamma_Q\right)$" ranged from 0.7395 to 0.9985, suggest strong performance. However, these values can be misleading since LP3 tends to emphasize central data points, overlooking extreme values in the tails (Figure 2a–d) [54]. Therefore, we used the ratio (R) of observed to estimated flood values as a more informative indicator: R > 1 indicates underestimation (poor performance), while R < 1 suggests overestimation (better performance) of flood quantiles.

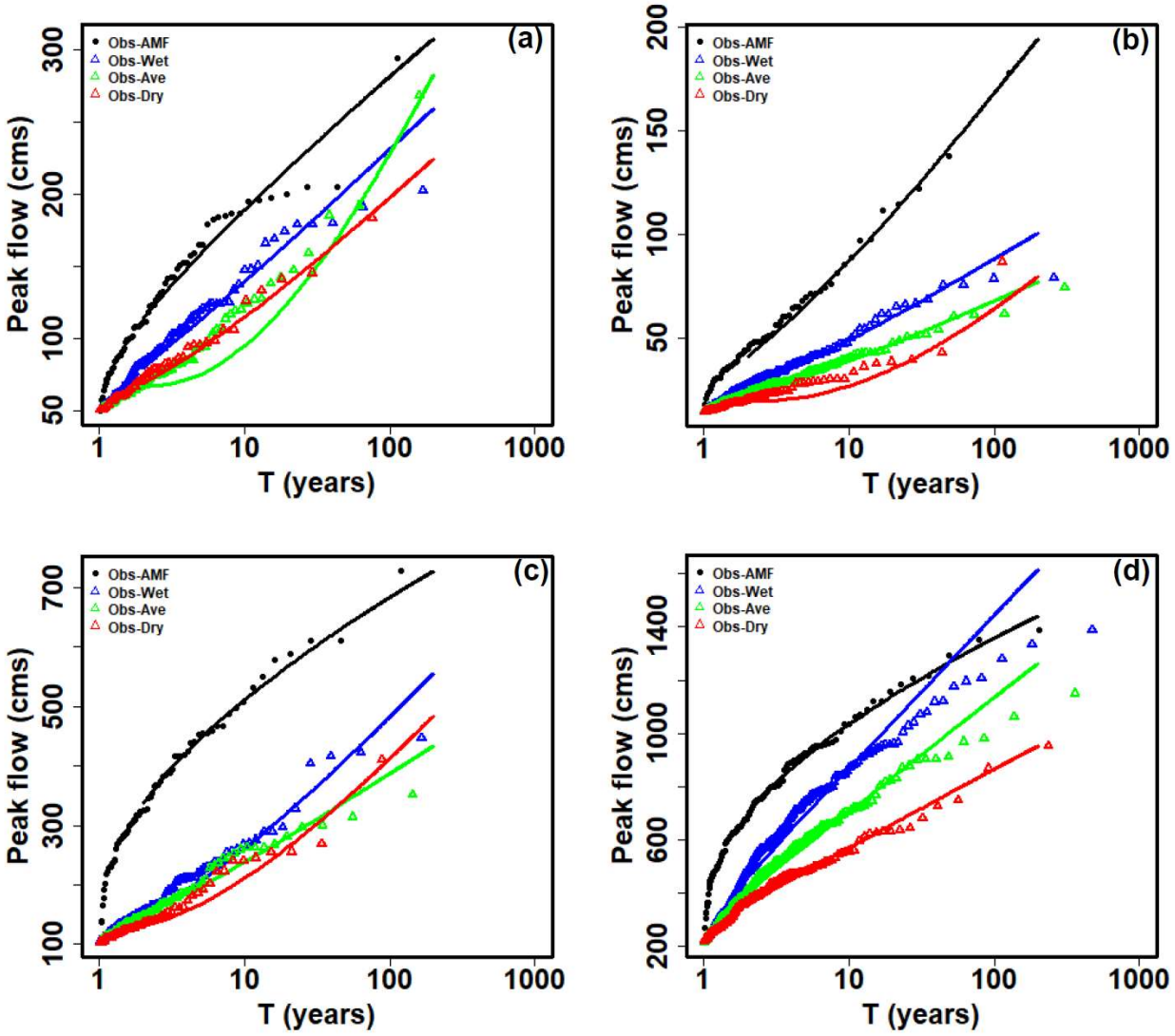

Figure 2. The flood frequency curves for selected sites: (**a**) USGS 01022500; (**b**) USGS 12488500; (**c**) USGS 12060500; and (**d**) USGS 12422500. These curves indicate the LP3 distribution fitted to the AMF (solid black line) and PDS of wet (blue), average

(green), and dry (red) years. The *x*-axis represents base-10 logarithm of return period in years, while the *y*-axis displays peak flow in cubic meters per second (cms). Depending on the region of interest, flooding events during average and dry years can exceed those observed during wet years.

Table 1. The range of Pearson cross-correlation values for $K_{P_i}(\gamma_Q)$ against Z_i as a result of goodness-of-fit test for LP3 fitted to either AMF or PDS of average, wet, or dry years.

Site	AMF	PDS-Average	PDS-Wet	PDS-Dry
Reference	0.9440–0.9982	0.8907–0.9938	0.8983–0.9937	0.8521–0.9933
Nonreference	0.8017–0.9985	0.8811–0.9961	0.7395–0.9980	0.7955–0.9440

4.2. Floods with Return Period of 2 Years

When LP3 was fitted to AMF and dry PDS data, 24–31% of reference and nonreference sites across the US provided reliable the 2-year flood estimates (R < 1, Table 2). For average and wet PDS, only 12–20% of sites had R < 1. Two regions—the west (Rio Grande, Lower Colorado, Great Basin, and Pacific Northwest) and the east (Lower Mississippi, Tennessee, Mid-Atlantic, and New England)—had more sites with R < 1 when LP3 was fitted to dry PDS (Figure 3a). It suggests that frequent 2-year floods may be better represented by low peak flows from dry year records. Investigating the link between atmospheric circulation patterns and streamflow variations in dry years could help clarify the mechanisms generating high-frequency floods in these regions [38,39,55–61].

Table 2. The number of sites where observed floods were reliably estimated (indicated by a ratio of observed to estimated flood quantiles less than one). The numbers in parentheses represent the percentage of sites with R < 1 out of the total number of sites.

Return Period (Years)	AMF				PDS-Average				PDS-Wet				PDS-Dry			
	Reference		Nonreference		Reference		Nonreference		Reference		Nonreference		Reference		Nonreference	
2	56	(26%)	472	(31%)	34	(20%)	171	(15%)	21	(15%)	128	(12%)	44	(25%)	292	(24%)
5	84	(39%)	672	(44%)	8	(5%)	68	(6%)	8	(6%)	51	(5%)	14	(8%)	103	(8%)
10	103	(47%)	774	(51%)	22	(13%)	195	(17%)	23	(16%)	201	(19%)	41	(23%)	242	(20%)
25	107	(49%)	806	(53%)	67	(39%)	482	(41%)	52	(36%)	454	(42%)	67	(38%)	455	(37%)
50	104	(48%)	752	(49%)	116	(67%)	775	(67%)	99	(69%)	711	(66%)	111	(63%)	756	(61%)
100	107	(49%)	707	(47%)	132	(77%)	880	(76%)	109	(76%)	807	(75%)	121	(69%)	873	(71%)
200	102	(47%)	693	(46%)	135	(78%)	927	(80%)	121	(85%)	848	(78%)	123	(70%)	902	(73%)
Total number of sites *	218		1520		172		1164		143		1082		176		1230	

* Out of a total 247 reference and 1781 nonreference sites with more than 70 years of peak flow records throughout the US. The number of sites in this table represents those where LP3 could provide flood quantiles estimates. For sites with β < 3, no flood quantiles estimates were available.

4.3. Floods with Return Period of 5 Years

With LP3 fitted to AMF, reliable estimates of 5-year flood events were achieved at 39% of reference sites and 44% of nonreference sites (Table 2). PDS based on average, wet, or dry years did not improve 5-year flood estimates across any HUC02 regions (Figure 3b). Regions such as the South-Atlantic-Gulf to Great Lakes and Pacific Northwest to the Upper Mississippi had significantly more sites where LP3 was well-fitted to AMF series, as shown by the dashed circles on Figure 3b.

Most 5-year flood events occurring in winter could be linked to increased Gulf of Mexico winter storms, which brought heavier precipitation as they moved northward, particularly during strong El Niño years [62–65]. In the central-to-west regions, a combination of several circulation patterns appears to influence flood-generating mechanisms [66–70]. McCabe and Wolock (2014) [71] found both positive and negative correlations between streamflow variations and large-scale climate patterns, including NINO3.4 sea surface temperatures, the Pacific Decadal Oscillation (PDO), the Atlantic Multi-decadal Oscillation (AMO), the Pacific North American Index (PNA), and the North Atlantic Oscillation (NAO).

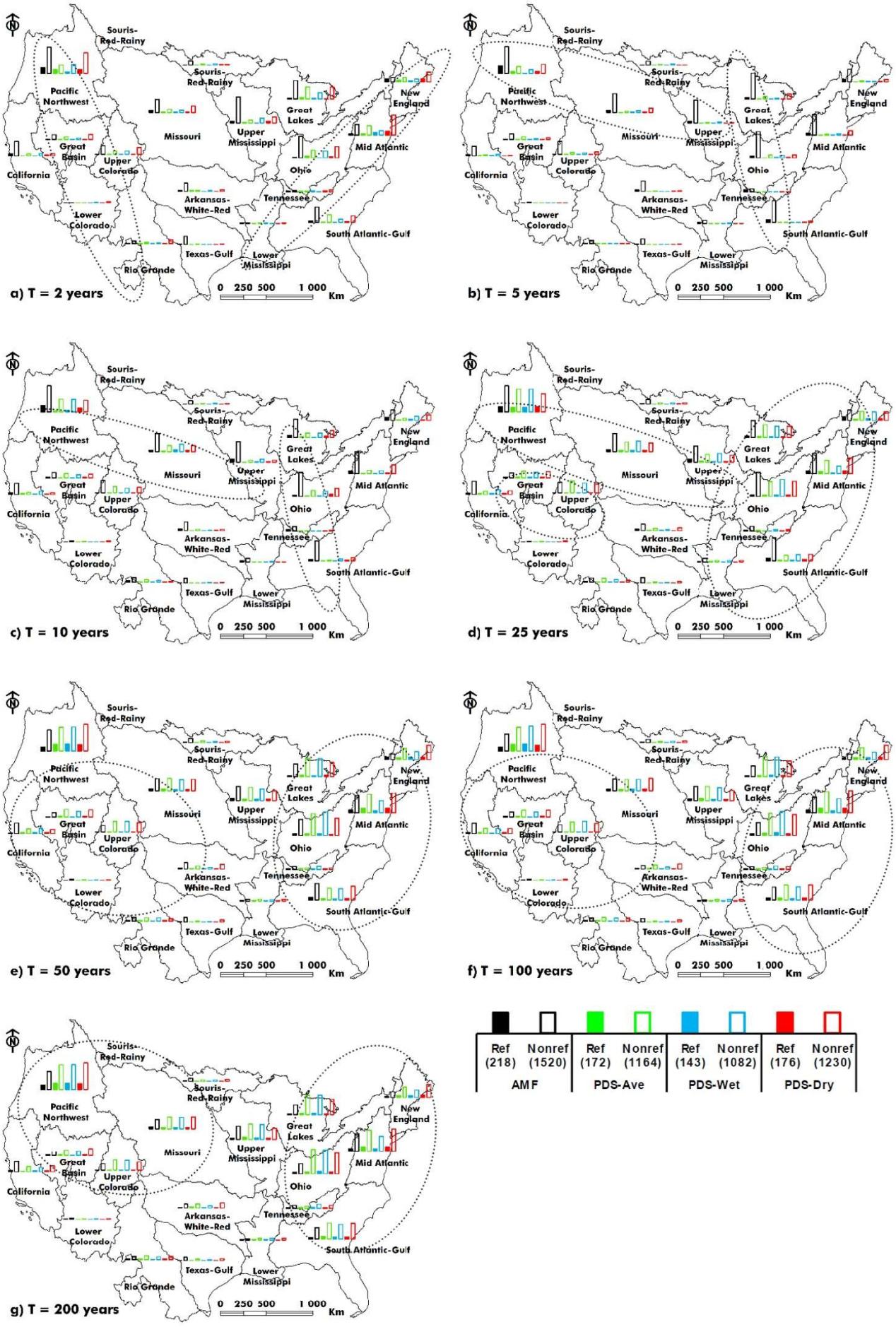

Figure 3. The number of reference and nonreference sites with R < 1 when LP3 was fitted to the AMF and PDS of average, wet, and dry years. Filled columns indicate the number of reference sites where LP3 showed better performance in estimating flood

quantiles. The relative height differences visually convey whether PDS outperformed AMF. Hollow columns provide similar information for nonreference sites. To maintain clarity and avoid overcrowding, detailed numerical values are provided in Table 2. Regions with specific patterns are indicated by dashed circles. The numbers in the legend represent the total number of study sites where LP3 could be fitted to their peak flow observations. For instance, LP3 was fitted to AMF at 218 reference and 1520 nonreference sites. The total number of reference and nonreference sites was 247 and 1781, respectively (see Figure 1).

4.4. Floods with Return Period of 10 Years

LP3 estimated 10-year flood events reliably at 47% of reference sites and 51% of nonreference sites when fitted to AMF (Table 2). None of the PDS derived from average, wet, or dry years improved these estimates. Similar to 5-year events, the South Atlantic-Gulf, Ohio, Great Lakes, Upper Mississippi, Missouri, and Pacific Northwest regions showed more sites with $R < 1$ than other US areas (dashed circles on Figure 3c). For 10-year floods, sites with $R < 1$ were nearly three times as common as for 5-year events when considering average, wet, or dry PDS (Table 2).

4.5. Floods with Return Period of 25 Years

Except for the New England, Mid Atlantic, and South Atlantic-Gulf regions, the number of reference sites with $R < 1$ was similar whether LP3 was fitted to AMF or PDS from average, wet, and dry years (Table 2). Two clusters emerged —along the East Coast (South Atlantic-Gulf, Mid Atlantic, New England, Ohio, and Great Lakes) and centrally to the West Coast (Upper Mississippi, Missouri, and Pacific Northwest)—where LP3 performed better with AMF than PDS (Figure 3d, dashed circles). None of the PDS improved the 25-year flood estimates, but using PDS resulted in more sites with $R < 1$ for 25-year floods compared to shorter return periods. Additionally, a new cluster appeared in the Great Basin and Upper Colorado regions, where PDS outperformed AMF for a larger number of nonreference sites (Figure 3d).

4.6. Floods with Return Period of 50 Years

For floods with return periods of 50, 100, and 200 years, the PDS significantly improved the estimation of flood quantiles. For 50-year floods, two distinct clusters were identified: one in the western regions (Missouri, Upper Colorado, Great Basin, and Pacific Northwest) and another in the eastern regions (Ohio, Great Lakes, Mid Atlantic, and New England) of the 105th meridian. In these areas, LP3 was better fitted to observed floods when using PDS information instead of AMF, as indicated by a higher number of sites with R values less than 1 (see Figure 3e and Table 2).

Since a 50-year flood occurs less frequently than 25- or 10-year floods, it appears that as the return period increases, the PDS developed from mean daily streamflow during wet or dry years, provides better flood quantile estimates than AMF (see Table 2). A comparison of daily precipitation across the US from 1950–1979 and 1980–2009 showed increases in both the intensity and frequency of light precipitation events ($1 \leq P < 10$ mm) for the two clusters identified on Figure 3e [67]. Furthermore, other water resources regions also experienced an increase in the number of sites where LP3 fit better to PDS than to AMF (see Table 2).

4.7. Floods with Return Periods of 100 and 200 Years

Similar to the findings for 50-year floods, PDS information derived from average, wet, or dry years increased the number of sites where LP3 reliably estimated 100- and 200-year floods, with the South Atlantic-Gulf region added to the eastern cluster (see Figure 3f,g, marked by dashed circles) (Table 2). It suggests that less frequent floods are better estimated using peak flow information from extreme wet or dry years, in addition to AMF data.

Higgins and Kousky (2013) [67] noted increases in moderate and heavy precipitation east of the 105th meridian, with no significant changes observed to the west. Since PDS derived from wet or dry years provided better flood quantile estimates than AMF in the identified clusters, there may be an increase in moderate to heavy rainfall events west of the 105th meridian, which warrants further investigation. Additionally, the occurrence of lower frequency floods with longer return periods could be influenced by variations in extreme phases of atmospheric circulation patterns over the Pacific and Atlantic oceans [39,69,72,73].

5. Summary and Conclusions

In this study, we hypothesized that the genesis of floods varies among average, wet, and dry years, as defined by anomalies from the long-term annual average. We fitted the LP3 distribution to the PDS of average, wet, and dry years,

alongside using the AMF, to assess their reliability in estimating flood quantiles. By distinguishing results from reference sites (total of 247) and nonreference sites (total of 1781), we aimed to understand how flood quantile estimates vary with the level of anthropogenic disturbances.

For high-frequency, 2-year flooding events—also recognized as the bankfull stage [7,74,75]—we found that the LP3 distribution fitted to the PDS of dry years provided a greater number of sites with reliable flood estimates ($R < 1$) in the eastern and western US (Figure 3a). Notably, the percentage of sites with $R < 1$ increased from reference to nonreference sites when LP3 was fitted to AMF. Conversely, the percentage decreased for nonreference sites when LP3 was fitted to PDS (Table 2).

For floods with return periods of 5–25 years, using AMF instead of PDS led to more reliable quantile estimates, particularly at nonreference sites (Figure 3b–d). When LP3 was fitted to AMF, the percentage of sites with $R < 1$ increased for nonreference sites. Distinguishing between site types showed no significant change in the percentage of sites with $R < 1$ when LP3 was fitted to the PDS of average, wet, or dry years (Table 2).

For less frequent floods with return periods of 50–200 years, primarily observed in two distinct clusters (the South Atlantic-Gulf, Ohio, Great Lakes, Mid Atlantic, and New England in the east; and Missouri, Upper Colorado, Great Basin, and Pacific Northwest in the west), the PDS derived from extreme wet and dry years outperformed AMF in estimating flood quantiles (Figure 3e–g). However, the percentage of sites with $R < 1$ varied between reference and nonreference sites, with a notable difference in the percentage of reference sites (85%) compared to nonreference sites (78%) when LP3 was fitted to the PDS of wet years (Table 2). This difference suggests estimating floods during wet years at nonreference sites (under both nonstationary climate conditions and anthropogenic disturbances) can be particularly challenging for less frequent 200-year flooding events.

Our findings challenge the assumption that wet years could consistently produce greater flooding than average or dry years across the US (Figure 3). Some regions experienced floods in wet years that surpassed those in average and dry years, while others exhibited the opposite trend (Figure 3b–d). This study enhances our understanding of the complexities involved in reliable flood quantile estimation by considering the PDS of average, wet, or dry years alongside AMF, tailored to specific regions across the conterminous United States.

Ultimately, these reliable and updated flood estimates can significantly improve infrastructure design, reservoir management strategies, and flood inundation mapping. Such improvements are essential for water managers as they navigate the challenges posed by a nonstationary climate and ongoing anthropogenic disturbances. Additionally, hydrologists and flood modelers can benefit from more reliable flood quantile estimates during model validation, verification, and calibration processes. Future research should investigate the influence of localized factors on flood behavior to refine estimation methods and enhance flood resilience strategies tailored to specific regions, considering both local and regional hydrology. While this paper focuses on the overall comparison of flood quantile estimation methods, a deeper exploration of these specific flood events, such as the changes in the proportion of stations under different fitting scenarios, could be the subject of future studies.

Supplementary Materials

The following supporting information can be found at: https://www.sciepublish.com/article/pii/347, The supporting information for reference (#247) and nonreference (#1781) sites are provided, with more than 70 years of peak flow data across the contiguous United States.

Acknowledgments

Authors would like to acknowledge and extend their gratitude for the support provided by Kansas State University for the current research. The work was conducted between 2018–2019, during Berton's tenure as a postdoctoral fellow and Rahmani's tenure as an assistant professor in the Department of Biological and Agricultural Engineering at Kansas State University.

Author Contributions

R.B.: Conceptualization, Methodology, Software, Validation, Formal Analysis, Investigation, Data Curation, Writing—Original Draft Preparation, Writing–Review & Editing, Visualization; V.R.: Conceptualization, Validation, Resources, Writing—Review & Editing, Supervision, Project Administration, Funding Acquisition.

Ethics Statement

Not applicable.

Informed Consent Statement

Not applicable.

Funding

This research was funded by the Department of Biological and Agricultural Engineering at Kansas State University through the contribution number of "19-102-J" of the Kansas Agricultural Experiment Station.

Declaration of Competing Interest

The authors declare that they have no known competing financial interests or personal relationships that could have appeared to influence the work reported in this paper. Additionally, the views expressed in this paper are those of the authors and do not necessarily reflect the official positions or opinions of their affiliated institutions.

References

1. Hoerling M, Eischeid J, Perlwitz J, Quan X-W, Wolter K, Cheng L. Characterizing Recent Trends in U.S. Heavy Precipitation. *J. Clim.* **2016**, *29*, 2313–2332. doi:10.1175/JCLI-D-15-0441.1.
2. Kim H, Villarini G. Higher emissions scenarios lead to more extreme flooding in the United States. *Nat. Commun.* **2024**, *15*, 237. doi:10.1038/s41467-023-44415-4.
3. Rahmani V, Harrington J. Assessment of climate change for extreme precipitation indices: A case study from the central United States. *Int. J. Climatol.* **2018**, *39*, 1013–1025. doi:10.1002/joc.5858.
4. Liang J, Liu X, AghaKouchak A, Ciais P, Fu B. Asymmetrical Precipitation Sensitivity to Temperature Across Global Dry and Wet Regions. *Earths Future* **2023**, *11*, e2023EF003617. doi:10.1029/2023EF003617.
5. Rodell M, Li B. Changing intensity of hydroclimatic extreme events revealed by GRACE and GRACE-FO. *Nat. Water* **2023**, *1*, 241–248. doi:10.1038/s44221-023-00040-5.
6. Westra S, Fowler HJ, Evans JP, Alexander LV, Berg P, Johnson F, et al. Future changes to the intensity and frequency of short-duration extreme rainfall. *Rev. Geophys.* **2014**, *52*, 522–555. doi:10.1002/2014RG000464.
7. Archfield SA, Hirsch RM, Viglione A, Blöschl G. Fragmented patterns of flood change across the United States. *Geophys. Res. Lett.* **2016**, *43*, 10232–10239. doi:10.1002/2016GL070590.
8. Berton R, Driscoll CT, Chandler DG. Changing climate increases discharge and attenuates its seasonal distribution in the northeastern United States. *J. Hydrol. Reg. Stud.* **2016**, *5*, 164–178. doi:10.1016/j.ejrh.2015.12.057.
9. Ivancic TJ, Shaw SB. Examining why trends in very heavy precipitation should not be mistaken for trends in very high river discharge. *Clim. Chang.* **2015**, *133*, 681–693. doi:10.1007/s10584-015-1476-1.
10. Knotters M, Bokhove O, Lamb R, Poortvliet PM. How to cope with uncertainty monsters in flood risk management? *Camb. Prisms Water* **2024**, *2*, e6. doi:10.1017/wat.2024.4.
11. Pirone D, Cimorelli L, Pianese D. The effect of flood-mitigation reservoir configuration on peak-discharge reduction during preliminary design. *J. Hydrol. Reg. Stud.* **2024**, *52*, 101676. doi:10.1016/j.ejrh.2024.101676.
12. Reinders JB, Munoz SE. Accounting for hydroclimatic properties in flood frequency analysis procedures. *Hydrol. Earth Syst. Sci.* **2024**, *28*, 217–227. doi:10.5194/hess-28-217-2024.
13. Sanchez GM, Petrasova A, Skrip MM, Collins EL, Lawrimore MA, Vogler JB, et al. Spatially interactive modeling of land change identifies location-specific adaptations most likely to lower future flood risk. *Sci. Rep.* **2023**, *13*, 18869. doi:10.1038/s41598-023-46195-9.
14. Najibi N, Devineni N. Recent trends in the frequency and duration of global floods. *Earth Syst. Dyn.* **2018**, *9*, 757–783. doi:10.5194/esd-9-757-2018.
15. Jean Louis M, Crosato A, Mosselman E, Maskey S. Effects of urbanization and deforestation on flooding: Case study of Cap-Haïtien City, Haiti. *J. Flood Risk Manag.* **2024**, *17*, e13020. doi:10.1111/jfr3.13020.
16. Torelló-Sentelles H, Marra F, Koukoula M, Villarini G, Peleg N. Intensification and Changing Spatial Extent of Heavy Rainfall in Urban Areas. *Earths Future* **2024**, *12*, e2024EF004505. doi:10.1029/2024EF004505.
17. Schedel JR, Schedel AL. Analysis of Variance of Flood Events on the U.S. East Coast: The Impact of Sea-Level Rise on Flood Event Severity and Frequency. *J. Coast. Res.* **2018**, *341*, 50–57. doi:10.2112/JCOASTRES-D-16-00205.1.
18. Zahmatkesh Z, Karamouz M. An uncertainty-based framework to quantifying climate change impacts on coastal flood vulnerability: Case study of New York City. *Environ. Monit. Assess.* **2017**, *11*, 567. doi:10.1007/s10661-017-6282-y.

19. Berghuijs WR, Woods RA, Hutton CJ, Sivapalan M. Dominant flood generating mechanisms across the United States: Flood Mechanisms Across the U.S. Geophys. *Res. Lett.* **2016**, *43*, 4382–4390. doi:10.1002/2016GL068070.
20. Mei X, Van Gelder PHAJM, Dai Z, Tang Z. Impact of dams on flood occurrence of selected rivers in the United States. *Front. Earth Sci.* **2017**, *11*, 268–282. doi:10.1007/s11707-016-0592-1.
21. Swetapadma S, Ojha CSP. A comparison between partial duration series and annual maximum series modeling for flood frequency analysis. In *Developments in Environmental Science*; Elsevier: Amsterdam, The Netherlands, 2023, pp. 173–192. doi:10.1016/B978-0-443-18640-0.00007-9.
22. Villarini G. On the seasonality of flooding across the continental United States. *Adv. Water Resour.* **2016**, *87*, 80–91. doi:10.1016/j.advwatres.2015.11.009.
23. Berton R, Rahmani V. Improving Low-Frequency Flood Estimation Using the Partial Duration Series Instead of the Annual Maximum Across the United States. *Adv in Hydro & Meteo*. **2024**, *1*, 14. doi:10.33552/AHM.2024.01.000523
24. Armstrong WH, Collins MJ, Snyder NP. Increased frequency of low-magnitude floods in New England. *J. Am. Water Resour. Assoc.* **2012**, *48*, 306–320.
25. Burn DH, Whitfield PH. Changes in cold region flood regimes inferred from long-record reference gauging stations. *Water Resour. Res.* **2017**, *53*, 2643–2658. doi:10.1002/2016WR020108.
26. Fischer S. Comparison of annual maximum series and flood-type-differentiated mixture models of partial duration series. *arXiv* **2021**, arXiv:2111.13393.
27. Swetapadma S, Ojha CSP. Technical Note: Flood frequency study using partial duration series coupled with entropy principle. *Hydrol. Earth Syst. Sci. Discuss.* **2021**, *2021*, 1–23. doi:10.5194/hess-2021-570.
28. Akinsanola AA, Chen Z, Kooperman GJ, Bobde V. Robust future intensification of winter precipitation over the United States. *Npj Clim. Atmos. Sci.* **2024**, *7*, 212. doi:10.1038/s41612-024-00761-8.
29. Liang Y, Gillett NP, Monahan AH. Climate Model Projections of 21st Century Global Warming Constrained Using the Observed Warming Trend. *Geophys. Res. Lett.* **2020**, *47*, e2019GL086757. doi:10.1029/2019GL086757.
30. Scafetta N. Impacts and risks of "realistic" global warming projections for the 21st century. *Geosci. Front.* **2024**, *15*, 101774. doi:10.1016/j.gsf.2023.101774.
31. England JF, Jr., Cohn TA, Faber BA, Stedinger JR, Thomas WO, Jr., Veilleux AG, et al. *Guidelines for Determining Flood Flow Frequency—Bulletin 17C (Report No. 4-B5), Techniques and Methods*; US Geological Survey: Reston, VA, USA, 2019. doi:10.3133/tm4B5.
32. Nied M, Pardowitz T, Nissen K, Ulbrich U, Hundecha Y, Merz B. On the relationship between hydro-meteorological patterns and flood types. *J. Hydrol.* **2014**, *519*, 3249–3262. doi:10.1016/j.jhydrol.2014.09.089.
33. Serago JM, Vogel RM. Parsimonious nonstationary flood frequency analysis. *Adv. Water Resour.* **2018**, *112*, 1–16. doi:10.1016/j.advwatres.2017.11.026.
34. Villarini G, Smith JA, Baeck ML, Krajewski WF. Examining Flood Frequency Distributions in the Midwest U.S. JAWRA J. *Am. Water Resour. Assoc.* **2011**, *47*, 447–463. doi:10.1111/j.1752-1688.2011.00540.x.
35. Bureau of Reclamation & USACE. Probabilistic Hydrologic Hazard Analysis. In *Best Practices in Dam and Levee Safety Risk Analysis, Training Manual*; The Bureau of Reclamation Technical Service Center and the U.S. Army Corps of Engineers Risk Management Center: Denver, Colorado, 2015; p. 20.
36. Griffis VW, Stedinger JR. Log-Pearson Type 3 Distribution and Its Application in Flood Frequency Analysis. I: Distribution Characteristics. *J. Hydrol. Eng.* **2007**, *12*, 482–491. doi:10.1061/(ASCE)1084-0699(2007)12:5(482).
37. Hu L, Nikolopoulos EI, Marra F, Anagnostou EN. Sensitivity of flood frequency analysis to data record, statistical model, and parameter estimation methods: An evaluation over the contiguous United States. *J. Flood Risk Manag.* **2020**, *13*, e12580. doi:10.1111/jfr3.12580.
38. Baxter S, Nigam S. A Subseasonal Teleconnection Analysis: PNA Development and Its Relationship to the NAO. *J. Clim.* **2013**, *26*, 6733–6741. doi:10.1175/JCLI-D-12-00426.1.
39. Berton R, Driscoll CT, Adamowski JF. The near-term prediction of drought and flooding conditions in the northeastern United States based on extreme phases of AMO and NAO. *J. Hydrol.* **2017**, *553*, 130–141. doi:10.1016/j.jhydrol.2017.07.041.
40. Wright DB, Yu G, England JF. Six decades of rainfall and flood frequency analysis using stochastic storm transposition: Review, progress, and prospects. *J. Hydrol.* **2020**, *585*, 124816. doi:10.1016/j.jhydrol.2020.124816.
41. Falcone J. *GAGES-II: Geospatial Attributes of Gages for Evaluating Streamflow (Vector Digital Data)*; U.S. Geological Survey: Reston, VA, USA, 2011.
42. Lins HF. *USGS Hydro-Climatic Data Network 2009 (HCDN–2009) (Fact Sheet)*; U. S. Geological Survey: Reston, VA, USA, 2012.
43. Hirsch RM, De Cicco LA. *User Guide to Exploration and Graphics for RivEr Trends (EGRET) and DataretRieval: R Packages for Hydrologic Data, Techniques and Methods*; U.S. Geological Survey: Reston, VA, USA, 2015.
44. Wickham H, François R, Henry L, Müller K. dplyr: A Grammar of Data Manipulation, R package version 0.7.6. 2018. Available online: https://dplyr.tidyverse.org/ (accessed on 1 April 2019).

45. Bezak N, Brilly M, Šraj M. Comparison between the peaks-over-threshold method and the annual maximum method for flood frequency analysis. *Hydrol. Sci. J.* **2014**, *59*, 959–977. doi:10.1080/02626667.2013.831174.
46. Lang M, Ouarda TBMJ, Bobée B. Towards operational guidelines for over-threshold modeling. *J. Hydrol.* **1999**, *225*, 103–117. doi:10.1016/S0022-1694(99)00167-5.
47. Fahim A, Jean R. The effect of certain restrictions imposed on the interarrival times of flood events on the Poisson distribution used for modeling flood counts. *Water Resour. Res.* **1983**, *19*, 481–485. doi:10.1029/WR019i002p00481.
48. Genz F, Luz LD. Distinguishing the effects of climate on discharge in a tropical river highly impacted by large dams. *Hydrol. Sci. J.* **2012**, *57*, 1020–1034. doi:10.1080/02626667.2012.690880.
49. Flynn KM. *Guidelines for Determining Flood flow Frequency—Bulletin 17B*; U.S. Geological Survey, Office of Water Data Coordination: Reston, VA, USA, 1982.
50. Whitfield PH. Floods in future climates: A review. *J. Flood Risk Manag.* **2012**, *5*, 336–365. doi:10.1111/j.1753-318X.2012.01150.x.
51. Stedinger JR, Vogel RM, Foufoula-Georgiou E. Frequency analysis of extreme events. In *Handbook of Hydrology*; Maidment DR, Ed.; McGraw-Hill, the University of Michigan: Ann Arbor, MI, USA, 1993; p. 1424.
52. Blom G. *Statistical Estimates and Transformed Beta-Variables*; John Wiley & Sons, Inc.: Hoboken, NJ, USA, 1958.
53. Lins HF, Slack JR. Seasonal and regional characteristics of US streamflow trends in the United States from 1940 to 1999. *Phys. Geogr.* **2005**, *26*, 489–501.
54. Alila Y, Mtiraoui A. Implications of heterogeneous flood-frequency distributions on traditional stream-discharge prediction techniques. *Hydrol. Process.* **2002**, *16*, 1065–1084. doi:10.1002/hyp.346.
55. Armstrong WH, Collins MJ, Snyder NP. Hydroclimatic flood trends in the northeastern United States and linkages with large-scale atmospheric circulation patterns. *Hydrol. Sci. J.* **2013**, *59*, 1636–1655. doi:10.1080/02626667.2013.862339.
56. Bradbury JA, Dingman SL, Keim BD. New England drought and relations with large scale atmospheric circulation patterns. *J. Am. Water Resour. Assoc.* **2002**, *38*, 1287–1299.
57. Durkee JD, Frye JD, Fuhrmann CM, Lacke MC, Jeong HG, Mote TL. Effects of the North Atlantic Oscillation on precipitation-type frequency and distribution in the eastern United States. *Theor. Appl. Climatol.* **2008**, *94*, 51–65. doi:10.1007/s00704-007-0345-x.
58. Enfield DB, Mestas-Nuñez AM, Trimble PJ. The Atlantic Multidecadal Oscillation and its relation to rainfall and river flows in the continental U.S. Geophys. *Res. Lett.* **2001**, *28*, 2077–2080. doi:10.1029/2000GL012745.
59. McCabe GJ, Dettinger MD. Decadal variations in the strength of ENSO teleconnections with precipitation in the western United States. *Int. J. Climatol.* **1999**, *19*, 1399–1410.
60. Najibi N, Devineni N, Lu M. Hydroclimate drivers and atmospheric teleconnections of long duration floods: An application to large reservoirs in the Missouri River Basin. *Adv. Water Resour.* **2017**, *100*, 153–167. doi:10.1016/j.advwatres.2016.12.004.
61. Steinschneider S, Lall U. Spatiotemporal Structure of Precipitation Related to Tropical Moisture Exports over the Eastern United States and Its Relation to Climate Teleconnections. *J. Hydrometeorol.* **2016**, *17*, 897–913. doi:10.1175/JHM-D-15-0120.1.
62. DeGaetano AT, Hirsch ME, Colucci SJ. Statistical Prediction of Seasonal East Coast Winter Storm Frequency. *J. Clim.* **2002**, *15*, 1101–1117. doi:10.1175/1520-0442(2002)015<1101:SPOSEC>2.0.CO;2.
63. Hirsch ME, DeGaetano AT, Colucci SJ. An East Coast Winter Storm Climatology. *J. Clim.* **2001**, *14*, 882–899. doi:10.1175/1520-0442(2001)014<0882:AECWSC>2.0.CO;2.
64. Kunkel KE, Angel JR. Relationship of ENSO to snowfall and related cyclone activity in the contiguous United States. *J. Geophys. Res. Atmos.* **1999**, *104*, 19425–19434. doi:10.1029/1999JD900010.
65. Ning L, Bradley RS. Winter precipitation variability and corresponding teleconnections over the northeastern United States. *J. Geophys. Res. Atmos.* **2014**, *119*, 7931–7945. doi:10.1002/2014JD021591.
66. Cai W, Santoso A, Wang G, Yeh S-W, An S-I, Cobb KM, et al. ENSO and greenhouse warming. *Nat. Clim. Chang.* **2015**, *5*, 849–859. doi:10.1038/nclimate2743.
67. Higgins RW, Kousky VE. Changes in Observed Daily Precipitation over the United States between 1950–79 and 1980–2009. *J. Hydrometeorol.* **2013**, *14*, 105–121. doi:10.1175/JHM-D-12-062.1.
68. Jiang R, Gan TY, Xie J, Wang N. Spatiotemporal variability of Alberta's seasonal precipitation, their teleconnection with large-scale climate anomalies and sea surface temperature. *Int. J. Climatol.* **2013**, *34*, 2899–2917. doi:10.1002/joc.3883.
69. Mallakpour I, Villarini G. Investigating the relationship between the frequency of flooding over the central United States and large-scale climate. *Adv. Water Resour.* **2016**, *92*, 159–171. doi:10.1016/j.advwatres.2016.04.008.
70. Steinschneider S, Ho M, Cook ER, Lall U. Can PDSI inform extreme precipitation?: An exploration with a 500 year long paleoclimate reconstruction over the U.S. *Water Resour. Res.* **2016**, *52*, 3866–3880. doi:10.1002/2016WR018712.
71. McCabe GJ, Wolock DM. Spatial and temporal patterns in conterminous United States streamflow characteristics. *Geophys. Res. Lett.* **2014**, *41*, 6889–6897. doi:10.1002/2014GL061980.
72. Coleman JSM, Budikova D. Eastern U.S. summer streamflow during extreme phases of the North Atlantic Oscillation. *J. Geophys. Res. Atmos.* **2013**, *118*, 4181–4193. doi:10.1002/jgrd.50326.

73. García-García D, Ummenhofer CC. Multidecadal variability of the continental precipitation annual amplitude driven by AMO and ENSO. *Geophys. Res. Lett.* **2015**, *42*, 526–535. doi:10.1002/2014GL062451.
74. Bieger K, Rathjens H, Allen PM, Arnold JG. Development and Evaluation of Bankfull Hydraulic Geometry Relationships for the Physiographic Regions of the United States. JAWRA J. *Am. Water Resour. Assoc.* **2015**, *51*, 842–858. doi:10.1111/jawr.12282.
75. He L, Wilkerson GV. Improved Bankfull Channel Geometry Prediction Using Two-Year Return-Period Discharge. *JAWRA J. Am. Water Resour. Assoc.* **2011**, *47*, 1298–1316. doi:10.1111/j.1752-1688.2011.00567.x.